

Extraction of the Neutron Electric Form Factor from Measurements of Inclusive Double Spin Asymmetries

V. Sulkosky,^{1,2} G. Jin,² E. Long,³ Y.-W. Zhang,⁴ M. Mihovilovic,⁵ A. Kelleher,¹ B. Anderson,⁶ D.W. Higinbotham,^{7,*} S. Širca,^{8,5} K. Allada,⁷ J.R.M. Annand,⁹ T. Averett,¹⁰ W. Bertozzi,¹ W. Boeglin,¹¹ P. Bradshaw,¹⁰ A. Camsonne,⁷ M. Canan,¹² G.D. Cates,² C. Chen,¹³ J.-P. Chen,⁷ E. Chudakov,⁷ R. De Leo,¹⁴ X. Deng,² A. Deur,⁷ C. Dutta,¹⁵ L. El Fassi,⁴ D. Flay,¹⁶ S. Frullani,^{17,†} F. Garibaldi,¹⁷ H. Gao,¹⁸ S. Gilad,¹ R. Gilman,^{7,4} O. Glamazdin,¹⁹ S. Golge,¹² J. Gomez,⁷ J.-O. Hansen,⁷ T. Holmstrom,²⁰ J. Huang,^{1,21} H. Ibrahim,²² C.W. de Jager,^{7,2,†} E. Jensen,²³ X. Jiang,²¹ M. Jones,⁷ H. Kang,²⁴ J. Katich,¹⁰ H.P. Khanal,¹¹ P. King,²⁵ W. Korsch,¹⁵ J. LeRose,⁷ R. Lindgren,² H.-J. Lu,²⁶ W. Luo,²⁷ P. Markowitz,¹¹ D. Meekins,⁷ M. Meziane,¹⁰ R. Michaels,⁷ B. Moffit,⁷ P. Monaghan,¹³ N. Muangma,¹ S. Nanda,⁷ B.E. Norum,² K. Pan,¹ D. Parno,²⁸ E. Piasezky,²⁹ M. Posik,¹⁶ V. Punjabi,³⁰ A.J.R. Puckett,¹ X. Qian,¹⁸ Y. Qiang,⁷ X. Qui,²⁷ S. Riordan,^{2,31,32} A. Saha,^{7,†} B. Sawatzky,⁷ M. Shabestari,² A. Shahinyan,³³ B. Shoenrock,³⁴ J. St. John,²⁰ R. Subedi,³⁵ W.A. Tobias,² W. Tireman,³⁴ G.M. Urciuoli,¹⁷ D. Wang,² K. Wang,² Y. Wang,³⁶ J. Watson,⁶ B. Wojtsekhowski,⁷ Z. Ye,¹³ X. Zhan,¹ Y. Zhang,²⁷ X. Zheng,² B. Zhao,¹⁰ and L. Zhu¹³

(Jefferson Lab Hall A Collaboration)

¹Massachusetts Institute of Technology, Cambridge, MA, 02139, USA

²University of Virginia, Charlottesville, VA, 22904, USA

³University of New Hampshire, Durham, NH, 03824, USA

⁴Rutgers University, New Brunswick, NJ, 08901, USA

⁵Jozef Stefan Institute, Ljubljana 1000, Slovenia

⁶Kent State University, Kent, OH, 44242, USA

⁷Thomas Jefferson National Accelerator Facility, Newport News, VA 23606, USA

⁸Faculty of Mathematics and Physics, University of Ljubljana, Ljubljana, 1000, Slovenia

⁹Glasgow University, Glasgow, G12 8QQ, Scotland, United Kingdom

¹⁰The College of William and Mary, Williamsburg, VA, 23187, USA

¹¹Florida International University, Miami, FL, 33181, USA

¹²Old Dominion University, Norfolk, VA, 23508, USA

¹³Hampton University, Hampton, VA, 23669, USA

¹⁴Universite di Bari, Bari, 70121 Italy

¹⁵University of Kentucky, Lexington, KY, 40506, USA

¹⁶Temple University, Philadelphia, PA, 19122, USA

¹⁷Istituto Nazionale Di Fisica Nucleare, INFN/Sanita, Roma, Italy

¹⁸Duke University, Durham, NC, 27708, USA

¹⁹Kharkov Institute of Physics and Technology, Kharkov 61108, Ukraine

²⁰Longwood University, Farmville, VA, 23909, USA

²¹Los Alamos National Laboratory, Los Alamos, NM, 87545, USA

²²Cairo University, Cairo, Giza 12613, Egypt

²³Christopher Newport University, Newport News, VA, 23606, USA

²⁴Seoul National University, Seoul, Korea

²⁵Ohio University, Athens, OH, 45701, USA

²⁶Huangshan University, People's Republic of China

²⁷Lanzhou University, Lanzhou, Gansu, 730000, People's Republic of China

²⁸Carnegie Mellon University, Pittsburgh, PA, 15213, USA

²⁹Tel Aviv University, Tel Aviv 69978, Israel

³⁰Norfolk State University, Norfolk, VA, 23504, USA

³¹University of Massachusetts, Amherst, MA, 01006, USA

³²Stony Brook University, Stony Brook, NY 11794, USA

³³Yerevan Physics Institute, Yerevan, Armenia

³⁴Northern Michigan University, Marquette, MI, 49855, USA

³⁵George Washington University, Washington, D.C., 20052, USA

³⁶University of Illinois at Urbana-Champaign, Urbana, IL, 61801, USA

Background: Measurements of the neutron charge form factor, G_E^n , are challenging due to the fact that the neutron has no net charge. In addition, measurements of the neutron form factors must use nuclear targets which require accurately accounting for nuclear effects. Extracting G_E^n with different targets and techniques provides an important test of our handling of these effects.

Purpose: The goal of the measurement was to use an inclusive asymmetry measurement technique to extract the neutron charge form factor at a four-momentum transfer of 1 (GeV/c)². This technique has very different

systematic uncertainties than traditional exclusive measurements and thus serves as an independent check of whether nuclear effects have been taken into account correctly.

Method: The inclusive quasi-elastic reaction ${}^3\overrightarrow{\text{He}}(\vec{\nu}, e')$ was measured at Jefferson Lab. The neutron electric form factor, G_E^n , was extracted at $Q^2 = 0.98 \text{ (GeV/c)}^2$ from ratios of electron-polarization asymmetries measured for two orthogonal target spin orientations. This Q^2 is high enough that the sensitivity to G_E^n is not overwhelmed by the neutron magnetic contribution, and yet low enough that explicit neutron detection is not required to suppress pion production.

Results: The neutron electric form factor, G_E^n , was determined to be $0.0414 \pm 0.0077 \text{ (stat)} \pm 0.0022 \text{ (syst)}$; providing the first high precision inclusive extraction of the neutron’s charge form factor.

Conclusions: The use of the inclusive quasi-elastic ${}^3\overrightarrow{\text{He}}(\vec{\nu}, e')$ with a four-momentum transfer near 1 $(\text{GeV/c})^2$ has been used to provide a unique measurement of G_E^n . This new result provides a systematically independent validation of the exclusive extraction technique results and implies that the nuclear corrections are understood. This is contrary to the proton form factor where asymmetry and cross-section measurements have been shown to have large systematic differences.

PACS numbers: 14.20.Dh, 13.40.Gp, 24.70.+s, 25.30.Bf

I. INTRODUCTION

Electromagnetic form factors describe the nucleon’s static electromagnetic structure and provide insight into understanding nucleons in terms of their fundamental degrees of freedom. Of the four electromagnetic form factors of the proton and neutron (G_E^p , G_M^p , G_E^n , and G_M^n), the measurement of G_E^n is particularly challenging due to its small value and the difficulty in obtaining a high-density “pure” neutron target. Extractions of neutron form factors have relied on measurements on light nuclei, such as the deuteron or ${}^3\text{He}$, where the neutron is bound inside the nucleus. Experimental methods that provide access to G_E^n include Rosenbluth separations from an unpolarized deuteron target [1, 2] and double-polarization measurements using either a polarized target [3–9] or an unpolarized target combined with a polarimeter to measure the polarization transfer to the recoiling neutron [10–13]. At low four-momentum-transfer-squared, Q^2 from 0.1 to 0.2 $(\text{GeV/c})^2$, inclusive quasi-elastic scattering from a polarized ${}^3\text{He}$ target was also tried [14, 15]. However, these early measurements yielded statistical uncertainties comparable with the extracted quantity; the sources of theoretical uncertainties were not investigated. In a later measurement, better statistical precision was obtained, and an extensive analysis of the systematic uncertainties was performed [16]. In that analysis, the large variation in the asymmetry predictions revealed a large model uncertainty at low Q^2 . The authors of that paper suggested that the extraction would be likely to succeed at higher Q^2 . We report in this paper an extraction of G_E^n at $Q^2 = 0.98 \text{ (GeV/c)}^2$ from measurements of the ratios of two asymmetries in the ${}^3\overrightarrow{\text{He}}(\vec{\nu}, e')$ reaction where the ${}^3\text{He}$ spin vectors aligned parallel and orthogonal to the electron beam direction.

II. METHODS

The measurements were performed at Jefferson Lab in experimental Hall A. A longitudinally polarized electron beam of 3.606 GeV was scattered from a gaseous polarized ${}^3\text{He}$ target. The beam current was between 10 μA and 15 μA , and the helicity of the beam was flipped at a frequency of 30 Hz. During the experiment, the beam charge asymmetry was minimized by a beam charge feedback system [17] and was controlled to be less than 100 parts per million (ppm) per 20–30 min time period. Interruptions of the beam were found to have negligible effects on the asymmetry. As a dedicated beam polarization measurement in Hall A was not conducted during the period the data were taken, the average beam polarization was determined from measurements taken in Hall B with a Møller polarimeter to be $(82 \pm 2.5)\%$ [18].

A polarized ${}^3\text{He}$ target was used as an effective polarized neutron target. The target, made of aluminosilicate glass, consisted of a pumping chamber and a target cell. The spherical pumping chamber was located above the cylindrical target cell and was connected to the target cell by a transfer tube. The ${}^3\text{He}$ nuclei were polarized via spin-exchange optical pumping of a Rb-K mixture [19]. The vapor of the alkali mixture was polarized in the pumping chamber, where the spin exchange with the ${}^3\text{He}$ nuclei occurred. The 40-cm-long target cell contained ${}^3\text{He}$ gas at 12 atm, which provided a luminosity of $10^{36} \text{ cm}^{-2}\text{s}^{-1}$. A small amount ($\simeq 2\%$ in number density) of N_2 gas was added to the target cell to absorb unwanted photons emitted from the Rb de-excitation process. With the aid of spectrally narrowed lasers that increase the light absorption efficiency [20], a significant improvement in target polarization was achieved compared to previous experiments with similar targets. The polarization of the cell was measured every 6 hours using nuclear magnetic resonance, calibrated using electron paramagnetic resonance [21] polarimetry. An average in-beam target polarization of $(50.2 \pm 2.5)\%$ was achieved. Additionally, a reference cell that could be filled with either ${}^3\text{He}$, N_2 , or H_2 gas, was used to determine the

* Corresponding author: doug@jlab.org

† Deceased

dilution factors for the unpolarized material in the cell.

The scattered electrons were detected in the Right High Resolution Spectrometer (RHRS) [22]. The RHRS was located at a forward angle of 17° with respect to the incident beam direction and its central momentum was set to 3.086 GeV/c. Thus, the momentum transfer to the target (\vec{q}) by an electron scattered into the center of the RHRS acceptance was pointing at an angle of 56° with respect to the incident beam direction. Scattered electrons traveled through the RHRS by passing through a pair of superconducting $\cos(2\theta)$ quadrupoles, a 6.6-m-long dipole magnet, and a third superconducting $\cos(2\theta)$ quadrupole. The detector package included: a pair of vertical drift chambers to determine the trajectory of a particle; two scintillator planes to provide the trigger; and a gas Cherenkov detector combined with a lead-glass electromagnetic calorimeter to separate electrons and pions. The spectrometer has a solid angle acceptance of 6 msr and a momentum acceptance of $\pm 4.5\%$. The spectrometer optics calibration resulted in the following resolutions: 6 mm in the vertex position along the beamline, 2×10^{-4} in relative momentum, 1.5 mrad in the out-of-plane angle and 0.5 mrad in the in-plane angle.

During the experiment, two sets of Helmholtz coils were used to align the ^3He spin vector either parallel or perpendicular to the beam direction. This enabled us to measure independently the asymmetries, A_{\parallel} and A_{\perp} , where the subscripts indicate the orientation of the ^3He spin vector with respect to the beam and in the horizontal lab-frame plane. The experimental physics asymmetries were calculated by

$$A = \frac{1}{P_e P_t f_{N_2}} \left(\frac{Y^+ - Y^-}{Y^+ + Y^-} \right), \quad (1)$$

where $Y^\pm = \frac{N^\pm}{Q^\pm LT^\pm}$ represents the normalized yield for beam helicity ± 1 , N^\pm is the number of detected scattered electrons, Q^\pm is the accumulated charge, and LT^\pm is the data acquisition live-time. P_e and P_t are the beam and target polarizations, respectively, and f_{N_2} is the dilution factor due to the admixture of N_2 gas in the target cell. The dedicated N_2 reference cell data were used to determine $f_{N_2} = (95 \pm 2)\%$. The measured asymmetries were calculated near the quasi-elastic peak for values of the Bjorken scaling variable $x_B = Q^2/(2M\omega)$ in the range $0.9 < x_B < 1.1$, where M is the mass of the nucleon and $\omega = E - E'$, where E (E') is the incident (scattered) electron energy.

Radiative corrections were calculated based on the formalism of Mo and Tsai [23] with the program RADCOR.F [24]. This code was updated to use the peaking approximation of Stein *et al.* [25] and can perform both external and internal corrections for unpolarized and polarized cross sections. For the polarized cross sections, the relative uncertainty of the radiative corrections was estimated to be 20% and up to 40%, when extrapolation from the model is involved [24]. The data from Ref. [26]

were used to build a model for the two helicity states and extrapolated to the kinematics of this paper. The model cross sections were then incorporated into the radiative correction procedure. The size of the corrections for the asymmetries varied from 8% to 14% across the x_B acceptance. Due to the assumptions used in building the model and the extrapolation, a conservative relative uncertainty of 50% was chosen for the radiative corrections, which results in a relative uncertainty of about 5% for the corrected asymmetries. Since these measurements were done at a moderate Q^2 and epsilon near unity, two-photon effects corrections should be small and thus have been neglected.

III. RESULTS

The A_{\parallel} and A_{\perp} inclusive ^3He asymmetries averaged over the spectrometer acceptance and after applying radiative corrections are shown in Fig. 1 with their values provided in Table I. The inner error bars represent the statistical uncertainties; the outer error bars show the combined statistical and systematic uncertainties. For the parallel asymmetry (A_{\parallel}), the statistical precision overwhelms the systematic uncertainty and, hence, the total error bar cannot be easily distinguished from the statistical error bar. The dominant experimental systematic uncertainties for the measured asymmetries are the uncertainty in the radiative corrections (5%), the target polarization (5%), the beam polarization (3%) and the dilution factor (2%), where all the uncertainties are relative to the asymmetry. The uncertainty due to inelastic backgrounds was not considered, since the statistical uncertainties dominate the total uncertainty. Within the statistical uncertainties, A_{\parallel} is almost constant across the chosen x_B range, whereas A_{\perp} exhibits a slight linear decrease with increasing x_B .

TABLE I. Parallel (A_{\parallel}) and transverse (A_{\perp}) asymmetries near the quasi-elastic peak versus x_B . The format for the asymmetries follows *central value* \pm *statistical uncertainty* \pm *systematic uncertainty*.

x_B	A_{\perp} (%)	A_{\parallel} (%)
0.925	$3.45 \pm 0.19 \pm 0.23$	$-0.35 \pm 0.17 \pm 0.02$
0.975	$3.29 \pm 0.20 \pm 0.23$	$-0.66 \pm 0.18 \pm 0.05$
1.025	$2.97 \pm 0.22 \pm 0.21$	$-0.55 \pm 0.20 \pm 0.04$
1.075	$2.86 \pm 0.26 \pm 0.20$	$-0.64 \pm 0.23 \pm 0.05$

To relate the measured asymmetries to G_E^n we used the formalism of Donnelly and Raskin [27] for scattering from a free spin-1/2 particle. The asymmetry for the $^3\text{He}(\vec{e}, e')$ reaction near the quasi-elastic peak can be written in terms of ^3He response functions as the ratio of the spin-averaged (Σ) and polarization (Δ) cross sections:

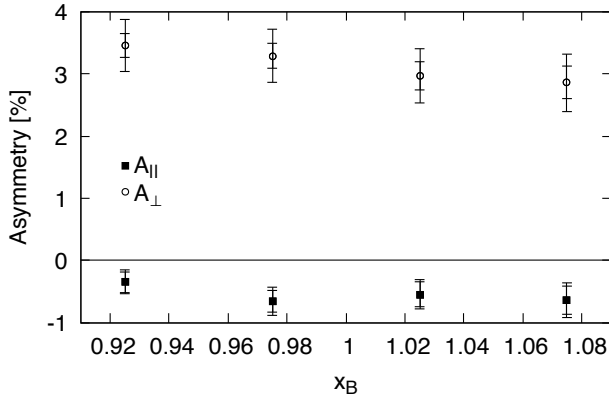


FIG. 1. Inclusive asymmetries from the ${}^3\text{He}(\vec{e}, e')$ reaction with the target spin parallel, ($A_{||}$), and transverse, (A_{\perp}), to the electron beam direction asymmetries near the quasi-elastic peak versus x_B . The inner (outer) error bars represent the statistical (statistical plus systematic) uncertainties.

$$A(\theta^*, \phi^*) = \frac{\Delta(\theta^*, \phi^*)}{\Sigma(\theta^*, \phi^*)} = -\frac{\cos\theta^* v_{T'} R_{T'}^{3\text{He}} + \sin\theta^* \cos\phi^* v_{TL'} R_{TL'}^{3\text{He}}}{v_L R_L^{3\text{He}} + v_T R_T^{3\text{He}}}, \quad (2)$$

where $R_{T'(TL')}^{3\text{He}}$ are the ${}^3\text{He}$ polarized transverse (transverse-longitudinal) response functions, $R_{T(L)}^{3\text{He}}$ are the ${}^3\text{He}$ unpolarized transverse (longitudinal) response functions, and the v 's are kinematic factors which are independent of beam and target polarizations. θ^* and ϕ^* are, respectively, the polar and azimuthal angles of the target polarization vector with respect to the three-momentum transfer \vec{q} . Thus, asymmetries measured with the target oriented parallel (perpendicular) to the electron beam correspond to $\theta^* = 56^\circ$ and $\phi^* = 0^\circ$ ($\theta^* = 34^\circ$ and $\phi^* = 180^\circ$).

Following the Plane-Wave-Impulse-Approximation (PWIA) calculation by Kievsky *et al.* [28], the polarized ${}^3\text{He}$ transverse (transverse-longitudinal) response functions $R_{T'(TL')}^{3\text{He}}$ near the quasi-elastic peak are written as

$$R_{T'}^{3\text{He}} = \frac{Q^2}{2qM} (2[G_M^p]^2 H_{T'}^p + [G_M^n]^2 H_{T'}^n), \quad (3)$$

$$R_{TL'}^{3\text{He}} = -\sqrt{2} (2G_M^p G_E^p H_{TL'}^p + G_M^n G_E^n H_{TL'}^n), \quad (4)$$

where the $H_S^{p(n)}$ represent the proton (neutron) contribution to the response functions with $S = T'$ or TL' . The proton form factors, G_E^p and G_M^p , as well as the neutron magnetic form factor G_M^n , were constrained by the world

data. The values of $H_S^{n(p)}$ were calculated in Ref. [28] using models for the nucleon polarizations and momentum distributions in the ${}^3\text{He}$ nuclei. These values are almost constant over a wide range of Q^2 . Thus, by measuring A for two sets of (θ^*, ϕ^*) at electron scattering angles and scattered electron momenta spanning the acceptance of the RHRS subject to the constraint that $0.9 < x_B < 1.1$, we obtain two linearly independent equations. The dependence on the ${}^3\text{He}$ unpolarized response functions can be removed by taking the ratio of $A(\theta^*, \phi^*)$ for two sets of (θ^*, ϕ^*) :

$$\frac{A(\theta_2^*, \phi_2^*)}{A(\theta_1^*, \phi_1^*)} = \frac{\cos\theta_2^* v_{T'} R_{T'}^{3\text{He}} + \sin\theta_2^* \cos\phi_2^* v_{TL'} R_{TL'}^{3\text{He}}}{\cos\theta_1^* v_{T'} R_{T'}^{3\text{He}} + \sin\theta_1^* \cos\phi_1^* v_{TL'} R_{TL'}^{3\text{He}}} \quad (5)$$

which can be solved for G_E^n .

The uncertainties in the ratios of asymmetries were dominated by the statistical uncertainty (18.5%) in the values of $A_{||}$. In these ratios, the absolute values of corrections such as the beam and target polarizations cancel to first order and only their relative changes during the measurement contribute to the uncertainty. We estimate that the uncertainties in the asymmetry ratio from the beam and target polarizations are $\simeq 3\%$ and $\simeq 1\%$, respectively. Similarly, the dilution factors cancel. The radiative corrections are correlated for the two measured asymmetries so that they also mostly cancel in the ratio. When the radiative corrections are varied within the uncertainties, we found the ratios of the asymmetries change by $\ll 1\%$; however, due to the assumptions made in their determination, we have taken 1% to be a conservative estimate of the uncertainty from this source. Finally, the measurement of the asymmetries is sensitive to the target polarization angle θ^* that has an uncertainty of $\pm 0.3^\circ$. This results in a 3% uncertainty in the ratio. We estimate the total experimental systematic uncertainty to be 4.5% for the ratios of the asymmetries.

The discussion up to this point has been based on the PWIA framework. Corrections to this approximation must be considered. The effects of final state interactions (FSI) were examined and found to decrease significantly with increasing Q^2 [29, 30]. The PWIA calculation mentioned previously [28] was used in earlier determinations of G_M^n in the range $Q^2 = 0.1 - 0.6$ (GeV/c) 2 from measurements of the $A_{T'}$ asymmetry made at Jefferson Lab [31]. The effects of FSI were greatly reduced above Q^2 of 0.5 (GeV/c) 2 , and for $Q^2 \geq 1$ (GeV/c) 2 FSI corrections are expected to fall as Q^{-4} . Corrections for meson-exchange currents (MEC) are expected to be negligible at the quasi-elastic peak [32] and to decrease exponentially as Q^2 increases, based on the observation in Ref. [31] as well as the calculations of Golak [33].

Within the context of PWIA, inclusion of the off-shell nature of the struck nucleon into the calculation of the electron-nucleon cross section requires a model of the nucleon current. In particular, a model for the contribution of the anomalous magnetic moment of the struck nucleon must be chosen. The CC1 and CC2 prescrip-

tions of De Forest [34] for off-shell cross sections were used to obtain the ^3He responses. In these two prescriptions the off-shell effects are incorporated into the electron kinematics using different approaches as outlined in ref. [34]. In the CC1 prescription the four-momentum transfer is determined solely by the electron kinematics. In the CC2 prescription the three-momentum transfer, \vec{q} , is determined by the electron kinematics and the energy transfer from the final energy and initial momentum of the struck nucleon. It is to be noted that in both cases energy-momentum and current conservation are violated as in both cases the nucleons are treated as free particles. PWIA calculations using these forms provide good agreement with the unpolarized ^3He response functions [28]. For the polarized responses, both prescriptions provide essentially the same result for $R_{TL'}$, while the results for $R_{T'}$ in general differ less than 2% over the range of $0.1 \leq Q^2 \leq 2$ (GeV/c) 2 . Due to these differences, only the results from CC1 were reported in Ref. [28]. Other prescriptions are available [35] but were not considered.

When x_B is near 1, the struck nucleon is almost at rest before absorbing the virtual photon. After absorbing the photon, it has a momentum almost equal to that of the virtual photon. In the kinematics of this paper, the struck nucleon has a relativistic kinetic energy. Hence, the inclusion of relativistic effects in the theoretical calculations is essential. The uncertainty due to these effects was estimated in Ref. [32]. A comparison was made within the Virtual Nucleon and Light Cone approximations, which are different treatments of the relativistic motion of bound nucleons as well as electromagnetic currents. The difference between the predictions made using these two approximations was found to be 1.2% at $Q^2 \simeq 1$ (GeV/c) 2 .

Parameterizations of the three undetermined electromagnetic form factors were used as inputs to calculate an asymmetry at each kinematic point over the measured angular and momentum acceptance of the RHRS. For G_M^n the high precision data from Ref. [36] were used, and the values for G_E^p and G_M^p were provided by Refs. [37, 38], which were extracted after applying the two-photon exchange corrections as done in [39]. The values and uncertainties for the form factors used in the extraction at the central value of Q^2 are presented in Table II. Taking into account the correlations between G_E^p and G_M^p , these uncertainties in the form factors lead to an uncertainty of 1.4% in the extracted value of G_E^n . The extraction of G_E^n is not limited by the uncertainties on the individual form factors. Examining Eq. (5) reveals that the proton contributions to the response functions are suppressed in ^3He , and hence, their uncertainties in the extraction of G_E^n are also suppressed. On the other hand, as Q^2 increases the uncertainty on G_M^n (2.1–2.6%) becomes important at $Q^2 = 2.6$ (GeV/c) 2 . Finally, the uncertainty on G_E^p grows linearly with Q^2 and adds an equal uncertainty in the extraction of G_E^n at this Q^2 .

Using Eq. (5), the central value of G_E^n was varied to fit the calculated ratio of asymmetries to the experimentally

TABLE II. The values and uncertainties for the form factors used in the extraction at $Q^2 = 0.98$ (GeV/c) 2 . The column δG_E^n provides the contributions to the systematic uncertainty of G_E^n from the input form factors to Eq. (2).

Form Factor	Value	δG_E^n
G_E^p/G_D	0.9413 ± 0.0094	3.0×10^{-4}
$\mu_p G_M^p/G_D$	1.0456 ± 0.0104	2.5×10^{-4}
$\mu_n G_M^n/G_D$	0.9953 ± 0.0225	1.9×10^{-4}

measured ratios. The value for G_E^n extracted at $Q^2 = 0.98$ (GeV/c) 2 is

$$G_E^n = 0.0414 \pm 0.0077 \pm 0.0022, \quad (6)$$

where the first (second) uncertainty is statistical (systematic). In Fig. 2, the present result for G_E^n is shown as the solid square along with selected world data and parametrizations. The extracted result is consistent with the world data, showing the feasibility of this method for values of Q^2 larger than 0.8 (GeV/c) 2 . It should be noted that the present data were acquired in only 2.5 days of running. As the extraction of G_E^n was not the principal focus of the measurements, the running time was divided evenly between the two target polarization orientations: parallel to the electron beam and perpendicular to the beam. Had the division of running time been optimized, with 90% (10%) of the time allocated to the parallel (perpendicular) orientation, the statistical uncertainty on G_E^n would be reduced from 0.0077 to 0.0026.

IV. SUMMARY

In summary, an extraction of G_E^n from inclusive polarized $^3\text{He}(\vec{e}, e')$ quasi-elastic asymmetry measurements was presented. This method of forming the ratio of inclusive asymmetries provides an important independent check of other measurements and has several advantages. Firstly, the systematic uncertainties associated with neutron detection [8] are avoided. Secondly, the sensitivity to certain unavoidable systematic errors (beam and target polarizations, dilution factors and radiative corrections) are greatly reduced due to first-order cancellations in the ratio of asymmetries. The final result at $Q^2 = 0.98$ (GeV/c) 2 of $G_E^n = 0.0414 \pm 0.0077 \pm 0.0019$ was found to be consistent with other extraction techniques. This is in contrast to the proton, where at this same Q^2 , systematic differences between form factor extraction techniques were revealed [41].

We thank the Jefferson Lab Physics and Accelerator Divisions. This work was supported in part by the U.S. National Science Foundation and by the U.S. Department of Energy. It is supported by DOE contract No.

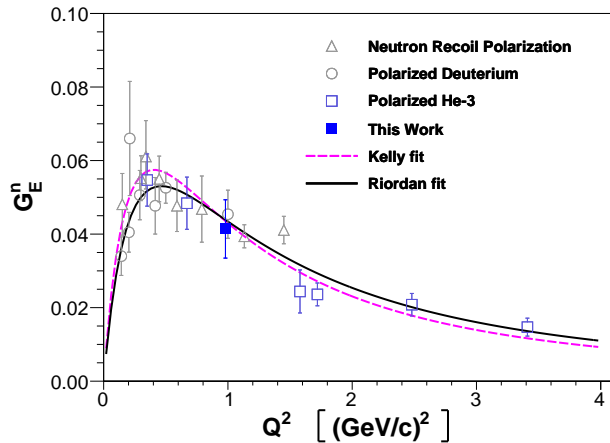


FIG. 2. The G_E^n value extracted from this experiment (solid square) and selected published data: open triangles [10–13], open circles [3–5], open squares [6–9] and parametrizations: Riordan *et al.* [8] and Kelly [40]. In regards to the polarized ^3He points, the solid square is from the inclusive reaction, whereas the open squares represent extracted results from experiments in which the neutron was tagged. The error bars show the statistical and the systematic uncertainties added in quadrature.

DE-AC05-06OR23177, under which Jefferson Science Associates (JSA), LLC, operates the Thomas Jefferson National Accelerator Facility.

-
- [1] S. Galster, H. Klein, J. Moritz, K. H. Schmidt, D. Wegener, and J. Bleckwenn, Nucl. Phys. **B32**, 221 (1971).
- [2] S. Platchkov *et al.*, Nucl. Phys. **A510**, 740 (1990).
- [3] I. Passchier *et al.*, Phys. Rev. Lett. **82**, 4988 (1999), arXiv:nucl-ex/9907012 [nucl-ex].
- [4] G. Warren *et al.* (Jefferson Lab E93-026), Phys. Rev. Lett. **92**, 042301 (2004), arXiv:nucl-ex/0308021 [nucl-ex].
- [5] E. Geis *et al.* (BLAST), Phys. Rev. Lett. **101**, 042501 (2008), arXiv:0803.3827 [nucl-ex].
- [6] J. Becker *et al.*, Eur. Phys. J. **A6**, 329 (1999).
- [7] J. Bermuth *et al.*, Phys. Lett. **B564**, 199 (2003), arXiv:nucl-ex/0303015 [nucl-ex].
- [8] S. Riordan *et al.*, Phys. Rev. Lett. **105**, 262302 (2010), arXiv:1008.1738 [nucl-ex].
- [9] B. S. Schlimme *et al.*, Phys. Rev. Lett. **111**, 132504 (2013), arXiv:1307.7361 [nucl-ex].
- [10] C. Herberg *et al.*, Eur. Phys. J. **A5**, 131 (1999).
- [11] M. Ostrick *et al.*, Phys. Rev. Lett. **83**, 276 (1999).
- [12] D. I. Glazier *et al.*, Eur. Phys. J. **A24**, 101 (2005), arXiv:nucl-ex/0410026 [nucl-ex].
- [13] B. Plaster *et al.* (Jefferson Laboratory E93-038), Phys. Rev. **C73**, 025205 (2006), arXiv:nucl-ex/0511025 [nucl-ex].
- [14] C. E. Jones-Woodward *et al.*, Phys. Rev. **C44**, R571 (1991).
- [15] A. K. Thompson *et al.*, Phys. Rev. Lett. **68**, 2901 (1992).
- [16] J. O. Hansen *et al.*, Phys. Rev. Lett. **74**, 654 (1995).
- [17] D. Androic *et al.* (G0), Nucl. Instrum. Meth. **A646**, 59 (2011), arXiv:1103.0761 [nucl-ex].
- [18] G. Jin, Ph.D. thesis, University of Virginia (2011).
- [19] E. Babcock, I. Nelson, S. Kadlecik, B. Driehuys, L. W. Anderson, F. W. Hersman, and T. G. Walker, Phys. Rev. Lett. **91**, 123003 (2003).
- [20] J. Singh, P. A. M. Dolph, W. A. Tobias, T. D. Averett, A. Kelleher, K. E. Mooney, V. V. Nelyubin, Y. Wang, Y. Zheng, and G. D. Cates, Phys. Rev. **C91**, 055205 (2015), arXiv:1309.4004 [physics.atom-ph].
- [21] M. V. Romalis *et al.*, *Polarized He-3 beams and gas targets and their application. Proceedings, 7th RCNP International Workshop, HELION'97, Kobe, Japan, January 20-24, 1997*, Nucl. Instrum. Meth. **A402**, 260 (1998).
- [22] J. Alcorn *et al.*, Nucl. Instrum. Meth. **A522**, 294 (2004).
- [23] L. W. Mo and Y.-S. Tsai, Rev. Mod. Phys. **41**, 205 (1969).
- [24] K. Slifer, Ph.D. thesis, Temple University (2004).
- [25] S. Stein, W. B. Atwood, E. D. Bloom, R. L. Cottrell, H. C. DeStaabler, C. L. Jordan, H. Piel, C. Y. Prescott, R. Siemann, and R. E. Taylor, Phys. Rev. **D12**, 1884 (1975).
- [26] K. Slifer *et al.* (E94010), Phys. Rev. Lett. **101**, 022303 (2008), arXiv:0803.2267 [nucl-ex].
- [27] T. W. Donnelly and A. S. Raskin, Annals Phys. **169**, 247 (1986).
- [28] A. Kievsky, E. Pace, G. Salme, and M. Viviani, Phys. Rev. **C56**, 64 (1997), arXiv:nucl-th/9704050 [nucl-th].
- [29] E. Pace, G. Salme, and G. B. West, Phys. Lett. **B273**, 205 (1991).
- [30] O. Benhar, Phys. Rev. Lett. **83**, 3130 (1999), arXiv:nucl-th/9908086 [nucl-th].
- [31] W. Xu *et al.* (Jefferson Lab E95-001), Phys. Rev. **C67**, 012201 (2003), arXiv:nucl-ex/0208007 [nucl-ex].
- [32] M. Sargsian, private communication (2012).
- [33] J. Golak, G. Ziener, H. Kamada, H. Witala, and W. Gloeckle, Phys. Rev. **C63**, 034006 (2001), arXiv:nucl-

- th/0008008 [nucl-th].
- [34] T. De Forest, Nucl. Phys. **A392**, 232 (1983).
 - [35] J. A. Caballero, T. W. Donnelly, and G. I. Poulis, Nucl. Phys. **A555**, 709 (1993).
 - [36] J. Lachniet *et al.* (CLAS), Phys. Rev. Lett. **102**, 192001 (2009), arXiv:0811.1716 [nucl-ex].
 - [37] S. Venkat, J. Arrington, G. A. Miller, and X. Zhan, Phys. Rev. **C83**, 015203 (2011), arXiv:1010.3629 [nucl-th].
 - [38] J. Arrington, private communication (2012).
 - [39] J. Arrington, W. Melnitchouk, and J. A. Tjon, Phys. Rev. **C76**, 035205 (2007), arXiv:0707.1861 [nucl-ex].
 - [40] J. J. Kelly, Phys. Rev. **C70**, 068202 (2004).
 - [41] M. K. Jones *et al.* (Jefferson Lab Hall A), Phys. Rev. Lett. **84**, 1398 (2000), arXiv:nucl-ex/9910005 [nucl-ex].